ANALYSIS OF THE DYNAMIC REGIME OF THE ACTUATING ELEMENT IN DISC BRAKES OF MINE HOISTING SYSTEMS

VALENTIN POPESCU[1], LAURA COJANU[2], FLORIN DUMITRU POPESCU[3]

Abstract: For extraction installations equipped with drum brakes, disadvantages such as the large size of active elements, heating, cooling, and deformation of passive elements during braking can be mitigated by using disc brakes. These brakes enable automation and the control of braking phenomena with the help of process computers. This paper proposes an analysis of the transient regime of the actuating element in disc brake systems for mining extraction machines from the perspective of systems theory.

Keywords: mine hoisting systems, brake discs, hydraulic parameters, actuating element

1. THEORETICAL CONCEPTS

The main components of a surface-based mine hoisting systems are shown in Figure 1. These include: the hoisting tower 1, the support structure (buttress) 2, the deflection sheaves 6, the hoisting cable 7, the hoisting vessels 8, and the hoisting machine, which consists of the cable winding mechanism 3 (in the presented case, in the form of drums), the reducer 4, and the drive motor 5.

The operating principle of mine hoisting systems can be summarized as follows: when the cable winding mechanism is set in motion by the drive motor, one branch of the traction cable winds onto the drum, lifting the transport vessel associated with that branch. Simultaneously, the cable on the other branch unwinds, causing the associated transport vessel to descend. When the two transport vessels reach the ramp levels, loading and unloading operations are performed, after which the transport cycle is repeated.

[1] *Ph.D. student Eng., University of Petroşani, vpv.popescu@gmail.com*
[2] *Ph.D. student Eng., University of Petroşani, cojanulaura@gmail.com*
[3] *Prof. Ph.D. Eng., University of Petroşani, fpopescu@gmail.com*

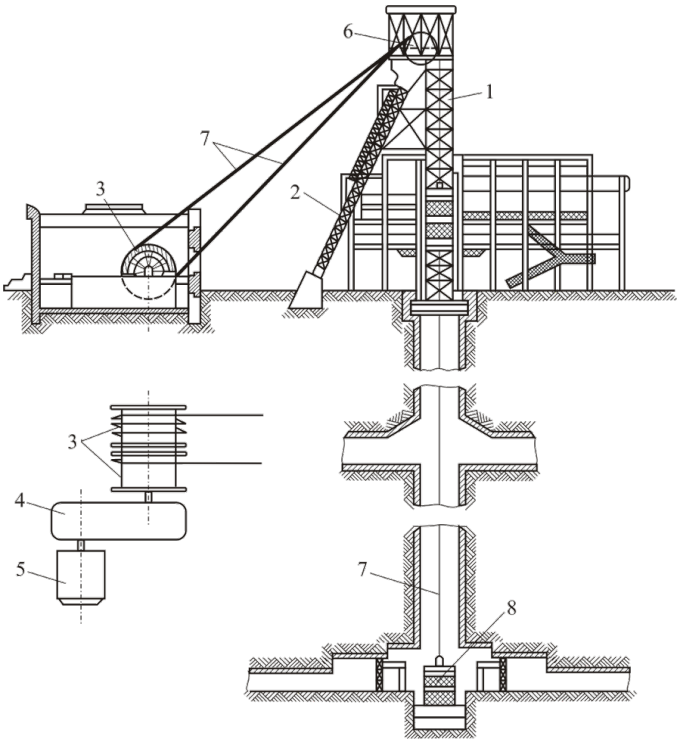

Fig. 1. The principle diagram of a surface-based hoisting systems

2. PRESENTATION OF THE TECHNICAL CHARACTERISTICS OF THE MINE HOISTING SYSTEM AND THE SOLUTION FOR MOUNTING THE BRAKE DISCS

Given that the MK 5x2 multi-cable mine hoisting system has been and continues to be one of the most widely used machines in the mines of the Jiu Valley, this hoisting installation was chosen as a reference model. For the design of the disc braking system, the following operating conditions of the MK 5x2 extraction installation were considered.

- Extraction capacity 1,4 mil tons/year
- Skip capacity 12 t
- Daily operating time (365 working days per year) 15 hours/day
- Hourly capacity 348 tons/hour
- Daily capacity 5220 tons/hour
- Maximum transport speed 14 m/s
- Maximum unbalanced static mass of the extraction machine 20 tons
- Drive power 2x1200 kW
- Supply voltage for electric motors 720 V c.c.

In Figure 2, the modification of the mine hoisting system drum required for the use of brake discs is shown, while Figure 3 presents the constructive characteristics of the disc as well as the placement of the active braking elements.

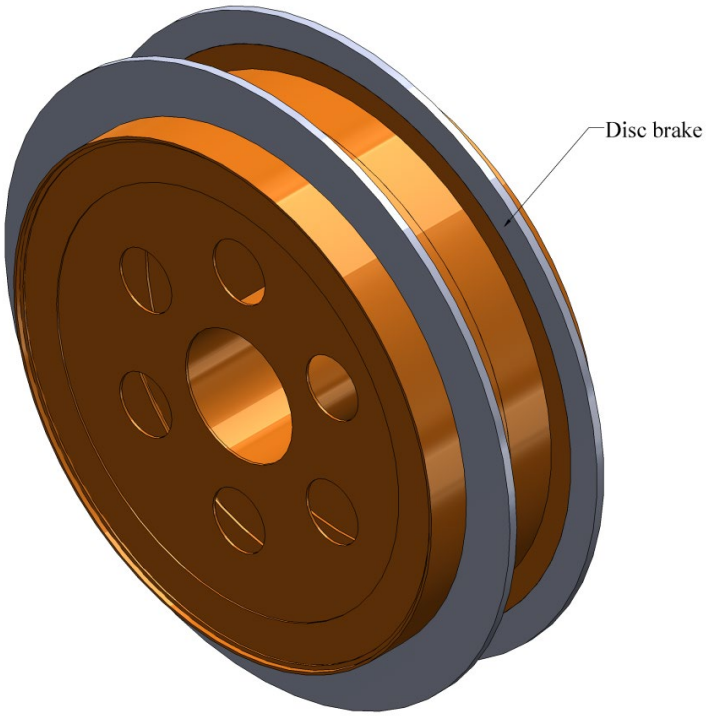

Fig. 2. Modification of the extraction machine drum

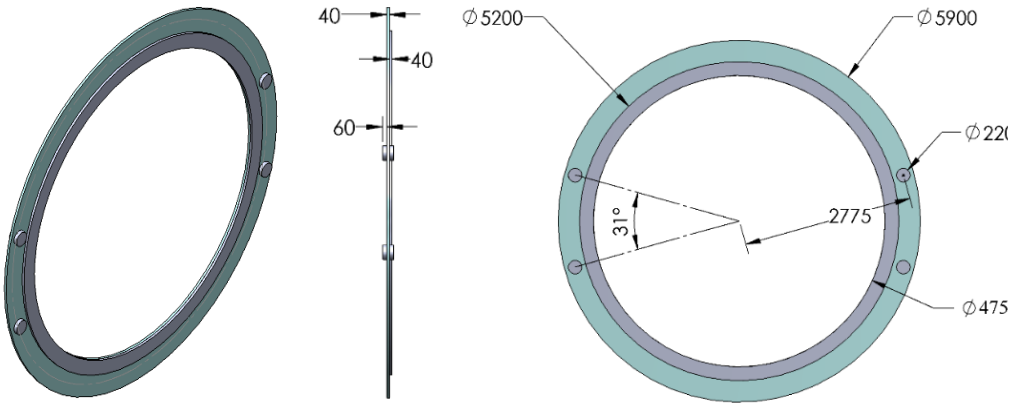

Fig. 3. Constructive characteristics of the disc and placement of the active braking elements

3. CALCULATION OF THE HYDRAULIC PARAMETERS OF THE ACTUATING ELEMENT

In Figure 4, the principle diagram of the braking hydraulic cylinder as an actuating element, coupled with a distributor, is presented.

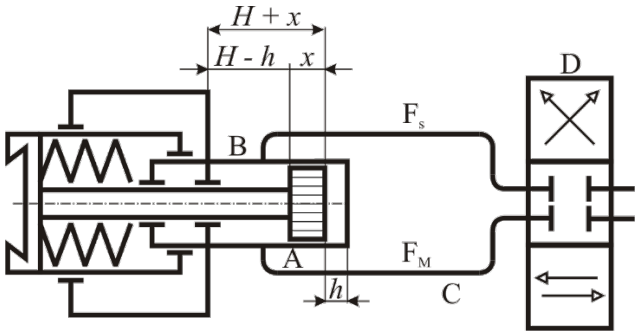

Fig. 4. Principle diagram of the hydraulic cylinder

The natural frequency and damping ratio are determined by the hydraulic capacity, the system mass, the oil volume in the hydraulic cylinder, as well as flow losses dependent on pressure and velocity.

To achieve high characteristic frequencies, which influence the dynamic stability of the hydraulic cylinder, the hydraulic capacity must be minimized. This requirement can be fulfilled by using a proportional distributor mounted in close proximity to the cylinder.

The natural frequency of the hydraulic cylinder with operational springs is given by the following relationship:

$$\omega_n = \sqrt{\frac{k_1}{m}} \quad \left[s^{-1}\right] \tag{1}$$

where:

k_1 =6734700 N/m is the static constant;

m =50,14 kg is the mass of the moving elements.

$$\omega_n = \sqrt{\frac{6734700}{50.14}} = 366 \left[s^{-1}\right]$$

The damping ratio is:

$$\xi = \frac{\frac{A^2}{k_3}}{2 \cdot \sqrt{k_1 \cdot m}} \tag{2}$$

where:

$$k_3 = \frac{\pi \cdot d_c^4}{128 \cdot \eta \cdot l_c} = \frac{\pi \cdot 0{,}01^4}{128 \cdot 3.72 \cdot 10^{-2} \cdot 0.1} = 6.6 \cdot 10^{-8} \left[m^5 / (N{\cdot}s) \right]$$

d_c =0,01 m is the diameter of the supply pipe;

l_c =0,1m is the length of the supply pipe;

A = 37,7·10^{-4} m^2 is the active area of the piston;

η=3,72·10^{-2} N·s/m^2 is the coefficient characterizing the dynamic viscosity.

$$\xi = \frac{\frac{37.7^2 \cdot 10^{-8}}{6.6 \cdot 10^{-8}}}{2 \cdot \sqrt{6734700 \cdot 50.14}} = 5.86 \cdot 10^{-3} < 1$$

Since the value of ξ is subunitary, it results that the system is underdamped.

The response time for underdamped system is calculated using the following relation:

$$t_r = \frac{\pi}{\omega_n \cdot \sqrt{1 - \xi^2}} \ [\text{s}] \tag{3}$$

$$\Rightarrow t_r = \frac{\pi}{366 \cdot \sqrt{1 - \left(5.86 \cdot 10^{-3}\right)^2}} = 8.6 \cdot 10^{-3} \ [\text{s}]$$

The determination of the calculation coefficients k_2, k_4 and k_5 is done by using the following relations:

$$k_2 = \frac{F_1}{p - p_0} \ \left[\text{m}^2 \right] \tag{4}$$

where:

F_1 =550 N ;

p =1000·10^4 N/m^2 is the maximum pressure in the cylinder.

p_0 =100·10^4 N/m^2 is the residual pressure in the cylinder.

$$k_2 = \frac{550}{(1000 - 100) \cdot 10^4} = 0.61 \cdot 10^{-4} \ \left[\text{m}^2 \right]$$

$$k_4 = \frac{H_{\max}}{Q_{\max}} \ \left[\text{s/ m}^2 \right] \tag{5}$$

where:

$H_{\max}$ = 0.004 m is the maximum stroke of the piston;

$Q_{\max}$ =160 l/min=2.6·10^{-3} m^3/s is the pump flow rate.

$$k_4 = \frac{0,004}{2.66 \cdot 10^{-3}} = 1.503 \left[\text{s/ m}^2 \right]$$

$$k_5 = \frac{N}{Q \cdot p} \tag{6}$$

where:

N is the hydraulic power.

Q is the oil flow rate in the cylinder, m^3/min.

$$N = \frac{Q \cdot p}{\eta_t} \tag{7}$$

where:

$_v = 3 \cdot 10^{-4}$ m/s is the piston speed in the cylinder;

$\eta_t = 0.92$ is the efficiency.

$$Q = \frac{A \cdot v}{\eta_t} = \frac{37.7 \cdot 10^{-4} \cdot 3 \cdot 10^{-4}}{0.92} = 123 \cdot 10^{-8} \ [\text{m}^3 / \text{s}]$$

$$N = \frac{123 \cdot 10^{-8} \cdot 1000 \cdot 10^4}{0.92} \approx 13.4$$

From (6) and (7), it results that:

$$k_5 = \frac{N}{Q \cdot p} = \frac{\frac{Q \cdot p}{\eta_t}}{Q \cdot p} = \frac{1}{\eta_t} = 1.087$$

The variation of pressure along the piston stroke will be:

$$p = \frac{k_4}{k_5} \cdot \frac{N}{H} = \frac{1,503}{1,087} \cdot \frac{13,4}{H} = \frac{18,53}{H} \ \left[\text{N/ m}^2 \right] \tag{8}$$

The variation of the flow rate as a function of the piston stroke is determined by the following relation:

$$Q = \frac{H}{k_4} = \frac{H}{1.503} \ \left[\text{m}^3 / \text{s} \right] \tag{9}$$

H and Q are the current values of the stroke and flow rate. For different values of H within the limits $\left(0 \ ... \ 0,004\right]$ m, the variation curves of pressure and flow rate are determined.

4. ANALYSIS OF THE TRANSIENT REGIME OF THE ACTUATING ELEMENT

For the study of the transient behavior of the hydraulic actuating element, the principle diagram shown in Figure 5 was analyzed.

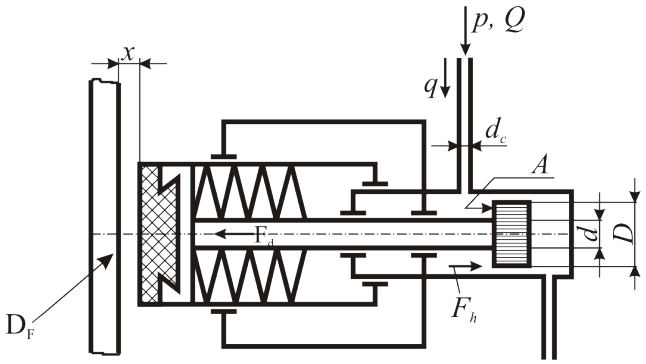

Fig.5. Principle diagram for the analysis of the transient regime of the actuating element

The oil pressure in the system acts on the piston surface, generating a hydraulic force that balances the resistance forces from the springs and the dynamic forces.

The equilibrium equation is:

$$F_h = F_1 + F_2 + F_a \ \left[\mathrm{N}\right] \tag{10}$$

where:

F_h is the hydraulic force in N:

$$F_h = A \cdot p - \frac{A^2}{k_3} \cdot \frac{\mathrm{d}x}{\mathrm{d}t} \ \left[\mathrm{N}\right] \tag{11}$$

where:

A = 37.7·10^{-4} m^2 is the active area of the piston;

k_3 = 6.6·10^{-4} $\left[\mathrm{m}^5/(\mathrm{N}\cdot\mathrm{s})\right]$;

p = 1000·10^4 N/m^2;

$$F_1 = k_2 \cdot (p - p_0) \ \left[\mathrm{N}\right] \tag{12}$$

k_2 =0,61·10^{-4} [m^2]

$$F_2 = m \cdot \frac{\mathrm{d}^2 x}{\mathrm{d}t^2} \le m \cdot a_{\max} \ \left[\mathrm{N}\right] \tag{13}$$

x is the current displacement of the piston, in m;

m is the mass of moving parts reduced to axis of the actuating element, in kg;

$a_{\max}$ is the maximum acceleration of the piston, in m/s^2.

$$a_{\max} = \frac{2 \cdot x_{\max}}{t_{\min}^2} \ \left[\mathrm{m/s}^2\right] \tag{14}$$

$x_{\max}$=H=0.004 m is the maximum stroke of the piston;
$t_{\min}$ is the minimum acceptable settling time, in s;
F_a is the forces in the disc springs.

$$F_a = k_1 \cdot \left(x + x_0\right) \left[\mathrm{N}\right] \tag{15}$$

x_0 is the deflection of the spring due to precompression ($x_0 \approx 0$);
k_1 6734700 N/m is the stiffness of the springs.

$$F_a = k_1 \cdot x \left[\mathrm{N}\right] \tag{16}$$

Thus, we obtain:

$$m \cdot \frac{\mathrm{d}^2 x}{\mathrm{d}t^2} + \frac{A^2}{k_3} \cdot \frac{\mathrm{d}x}{\mathrm{d}t} + k_1 \cdot x = A \cdot p - k_2 \cdot (p - p_0) \tag{17}$$

For a variation Δp of the pressure, equation (17) takes the following form:

$$m \cdot \frac{\mathrm{d}^2 x}{\mathrm{d}t^2} + \frac{A^2}{k_3} \cdot \frac{\mathrm{d}x}{\mathrm{d}t} + k_1 \cdot x = A \cdot \Delta p - k_2 \cdot (\Delta p - p_0) \tag{18}$$

The corresponding transfer function is:

$$T(s) = \frac{1}{m \cdot s^2 + \frac{A_2^2}{k_3} \cdot s + 1} \tag{19}$$

$$T(s) = \frac{1}{50{,}14 \cdot s^2 + \frac{37{,}7^2 \cdot 10^{-8}}{6{,}6 \cdot 10^{-8}} \cdot s + 1} = \frac{1}{50{,}14 \cdot s^2 + 215 \cdot s + 1}$$

Analyzing the differential equation of the dynamic behavior of the hydraulic cylinder, it is observed that the real part is composed of three terms that oppose the input variable represented by the oil pressure:

- the inertial term, which is proportional to the acceleration of the piston;
- the damping term, which is proportional to the velocity;
- the elastic term, which is proportional to the displacement of the piston.

By substituting the previously determined values, equation (18) becomes:

$$50{,}14 \cdot \frac{d^2 x}{dt^2} + 215 \cdot \frac{dx}{dt} + 6734700 \cdot x = 37{,}7 \cdot 10^{-4} \cdot \Delta p - 0{,}61 \cdot 10^{-4} \cdot \left(\Delta p - 100 \cdot 10^4\right) \tag{20}$$

By substituting the values of the natural frequency and damping ratio into equation (18), the following is obtained:

$$m \cdot \left(\frac{\mathrm{d}^2 x}{\mathrm{d}t^2} + 2 \cdot \xi \cdot \omega_n \cdot \frac{\mathrm{d}x}{\mathrm{d}t} + \omega_n^2 \cdot x \right) = A \cdot \Delta p - k_2 \cdot (\Delta p - p_0) \tag{21}$$

where:

ξ is the damping ratio;

ω_n is the natural frequency of the hydraulic cylinder;

The transfer function of the actuating element can be written in the form:

$$T(s) = \frac{1}{\left(\frac{s}{\omega_n} \right)^2 + 2 \cdot \xi \cdot \left(\frac{s}{\omega_n} \right) + 1} \tag{22}$$

The real part of the response is given by the roots r_1 and r_2.

$$r_{1,2} = -\xi \cdot \omega_n \pm \omega_n \cdot \sqrt{\xi^2 - 1}$$

For undamped system, where $\xi < 1$ we have:

$$x = e^{-\alpha t} \cdot \left[C_1 \cdot \sin(\omega_n t) + C_2 \cdot \cos(\omega_n t) \right] = k_c \cdot e^{-\xi \varpi_n t} \cdot \cos\left(\omega_n \cdot \sqrt{1 - \xi^2 \cdot t - \psi} \right) \tag{23}$$

where:

$$\psi = \arccos \sqrt{1 - \xi^2}$$

The system's response to a unit step input signal depends on ξ. Thus, for $\xi < 1$ we have the following relation:

$$x = \frac{k_1}{k_2} \cdot \left[1 - \frac{1}{\sqrt{1 - \xi^2}} \cdot e^{-\xi \varpi_n t} \cdot \cos(\omega_n t - \psi) \right] \tag{24}$$

The system's response to a sinusoidal signal of type $x = sin(\omega t)$ was analyzed using the transfer function, where $s = \mathrm{j}\omega$ was substituted.

$$T(\mathrm{j}\omega) = \frac{1}{\mathrm{j}\left(\frac{2 \cdot \xi \cdot \omega}{\omega_n} \right) + \left[1 - \left(\frac{\omega}{\omega_n} \right)^2 \right]} = \frac{b}{a^2 + b^2} - \mathrm{j} \frac{a}{a^2 + b^2} \tag{25}$$

The amplitude ratio is given by the following relation:

$$\left|\frac{\mathrm{x}}{\Delta \mathrm{p}}\right|=\frac{1}{\sqrt{\mathrm{a}^2+\mathrm{b}^2}}=\frac{1}{\sqrt{\left(\frac{2\cdot\xi\cdot\omega}{\omega_{\mathrm{n}}}\right)^2+\left[1-\left(\frac{\omega}{\omega_{\mathrm{n}}}\right)^2\right]^2}} \tag{26}$$

Analyzing the attenuation-frequency characteristics, it is observed that the output amplitude can tend to infinity in case of resonance $\left(\omega=\omega_n\right)$, but only if $\xi=0$.

For ξ subunitary, the increase in amplitude at resonance is limited according to the following relation:

$$\left|\frac{x}{\Delta p}\right|=\frac{1}{2\cdot\xi}\Rightarrow|\Delta p|=2\cdot\xi|x| \tag{27}$$

The phase shift ϕ of the response is also determined from the transfer function:

$$\phi=-\arctan\frac{a}{b}=-\arctan\frac{\frac{2\cdot\xi\cdot\omega}{\omega_n}}{1-\left(\frac{\omega}{\omega_n}\right)^2} \tag{28}$$

The system's response to a unit step signal is given by:

$$\Psi=\arccos\sqrt{1-\left(5{,}86\cdot10^{-3}\right)^2}=0{,}0086\left[\mathrm{rad}\right]$$

$$\Delta p=2\cdot\xi\cdot\frac{k_1}{k_2}\cdot\left[1-\frac{1}{\sqrt{1-\xi^2}}\cdot e^{-\xi\omega_n t}\cdot\cos\left(\omega_n t-\Psi\right)\right] \tag{29}$$

$$\Delta p=4{,}81\cdot\left[1-e^{-2{,}14\cdot t}\cdot\cos\left(366\cdot t-0{,}0086\right)\right]$$

In Table 1, the value of are presented as a function of time, while in Figure 6, the graph of pressure variation as a function of time is shown.

Tabel 1. **The value of** Δp

t [s]	0,01	0,02	0,03	0,04	0,05	0,06	0,07	0,08	0,09	0,10
Δp [N/m^2]	101	184	255	313	360	400	432	458	479	496

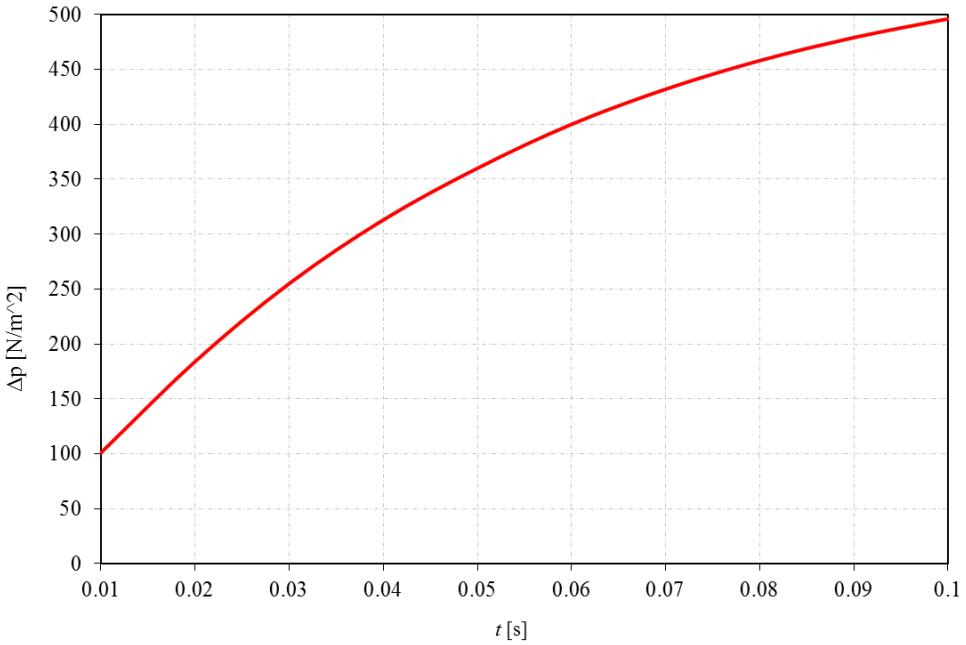

Fig. 6. Time variation of pressure

The amplitude ratios is:

$$\frac{x}{\Delta p} = \frac{1}{\sqrt{\left(\frac{2 \cdot 5{,}53 \cdot 10^{-2}}{363}\right) \cdot \omega^2 + 1 - \left(\frac{1}{363}\right)^2 \cdot \omega^2}}$$

$$\frac{x}{\Delta p} = \frac{1}{\sqrt{1 + 2{,}89 \cdot 10^{-4} \omega^2 + 5{,}76 \cdot 10^{-11} \omega^4}}$$

The variation in the amplitude ratio is shown in Table 2, and the graph of this variation is shown in Figure 7.

Table 2. **The variation in the amplitude ratio**

ω [rad/s]	100	200	300	400	500	600	700	800	900	1000
$x / \Delta p$	0,983	0,909	0,76	0,58	0,433	0,324	0,248	0,194	0,156	0,127

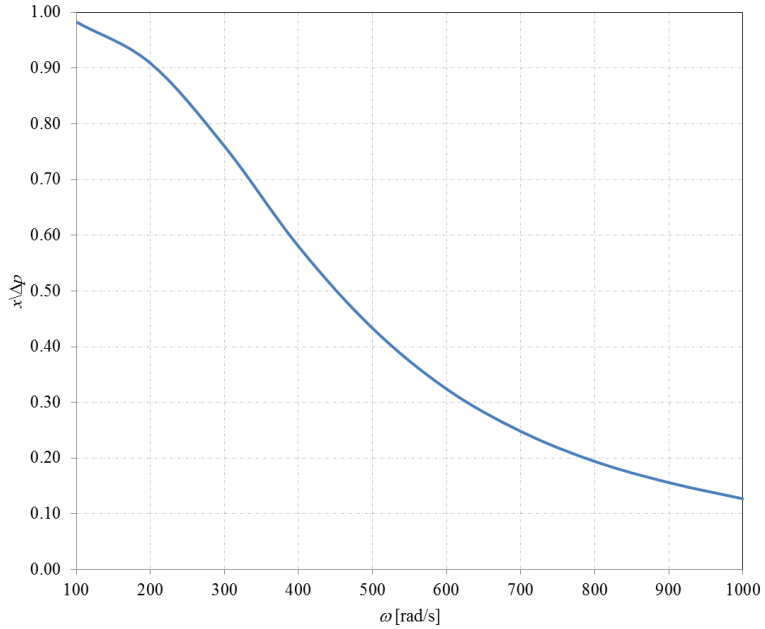

Fig. 7. Variation of the ratio $x / \Delta p$

The phase shift of the response is:

$$\phi = -\arctan \frac{\frac{2 \cdot 5{,}86 \cdot 10^{-3}}{366} \cdot \omega}{1 - \left(\frac{1}{366}\right)^2 \cdot \omega^2} = -\arctan \frac{3{,}2 \cdot 10^{-5} \cdot \omega}{1 - 7{,}46 \cdot 10^{-6} \cdot \omega^2}$$

For the representation of the phase shift ϕ depending on the pulsation ω, a program in C language has been developed. The screenshot of the phase shift obtained with the help of the program is shown in Figure 8.

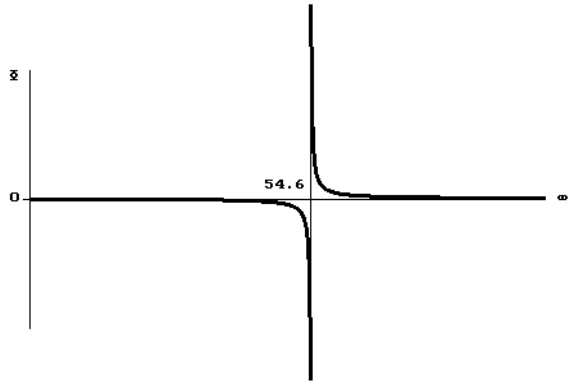

Fig. 8. Variation of response phase shift as a function of angular frequency

The lower the damping ratio, the faster the system's response to the variation in the input size, increasing observability and reducing the degree of stability.

If in the relation of the transfer function in its complex form:

$$T(\mathrm{j}\omega) = \frac{b}{a^2 + b^2} - \mathrm{j}\frac{a}{a^2 + b^2} \tag{30}$$

It is noted: $\frac{b}{a^2 + b^2} = x$ şi $\frac{a}{a^2 + b^2} = y$. To remove the parameter ω between x and y and obtain the mathematical form of the transfer place (Nyquist's place) proceed as follows:

$$x^2 - x + y^2 - \frac{y^2}{4 \cdot \xi^2 \cdot \left(x^2 + y^2\right)} = 0 \tag{31}$$

The system will be stable if, following the graphical representation, the coordinate point (-1; 0) remains to the left of the curve for any value of ξ>0.

To determine the transfer location, the transfer function (30) is used in the form:

$$T(j\omega) = \frac{1}{m \cdot (\mathrm{j}\omega)^2 + \frac{A^2}{k_3} \cdot (\mathrm{j}\omega) + k_1} \tag{32}$$

Using the known parameters, the curve of the transfer site was drawn by means of a program written in the C language.

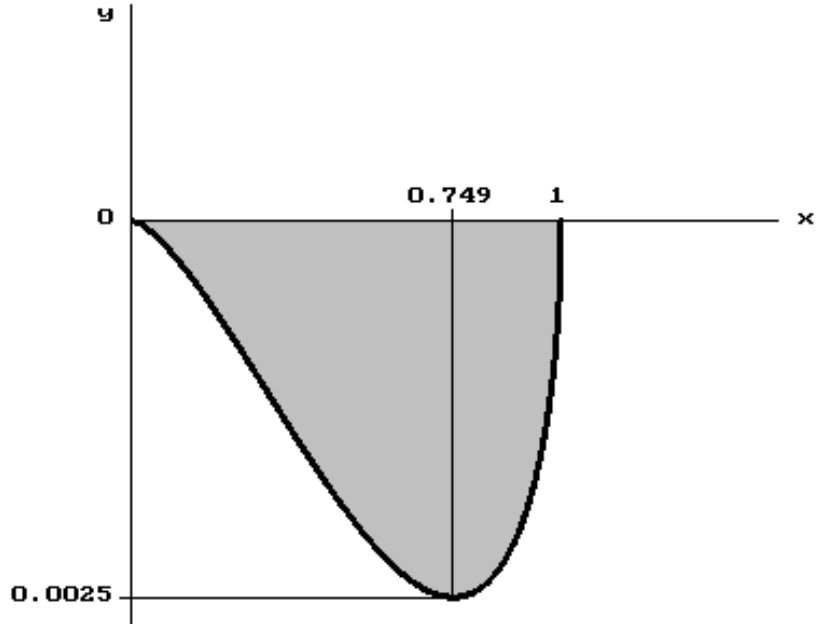

Fig. 9. The transfer locus graph

CONCLUSIONS

Given that during each extraction cycle multiple braking and un-braking operations occur, both during acceleration and deceleration periods, the hydraulic braking elements operate almost continuously in transient mode. For this reason, it was necessary to perform a dynamic behavior analysis of the braking element.

In this context, the mathematical model of the element coupled with a proportional distributor was studied, and the characteristic operating equations, time constants, amplification factors, damping ratio, and transfer function were determined.

The hydraulic parameters of the braking element were determined. For the working pressure in the hydraulic system, a value of 100 N/m2 was adopted.

Using the Nyquist stability criterion and plotting the transfer locus based on the calculated coordinates, it was found that the system behaves stably in transient mode.

REFERENCES

[1]. Popescu, F.D.; Radu, S.M.; Andraș, A.; Brînaș, I.; Budilică, D.I.; Popescu, V. Comparative Analysis of Mine Shaft Hoisting Systems' Brake Temperature Using Finite Element Analysis (FEA). *Materials* **2022**, *15*, 3363. https://doi.org/10.3390/ma15093363

[2]. Andraș, A., Brînaș, I., Radu, S.M., Popescu, F.D., Popescu, V., Budilică, D.I. *Investigation of the Thermal Behaviour for the Disc-Pad Assembly of a Mine Hoist Brake Using COMSOL Multiphysics.* Acta Tech. Napoc.-Ser. Appl. Math. Mech. Eng. 64, 227–234, 2021.

[3]. Popescu, F.D., Radu, S.M., Andras, A., Brinas, I.K. *A grafo-numeric method of determination of the operation power of the rotor of EsRc-1400 bucket wheel excavator using computer simulation in SolidWorks.* MATEC Web Conf. 290, 04007, 2019.

[4]. Mitran, I., Popescu, F.D., Nan, M.S., Soba, S.S. *Possibilities for Increasing the Use of Machineries Using Computer Assisted Statistical Methods*, WSEAS Transactions on Mathematics, Issue 2, Volume 8, February 2009.

[5]. Popescu, F. D., Radu, S. M., Andras, A., Kertesz (Brînaș), I. *Simulation of the frequency response of the ERC 1400 Bucket Wheel Excavator boom, during the excavation process*, New Trends in Production Engineering, Vol. 2, Issue 1, pp. 153-167, 2019.

[6]. Radu, S.M.; Popescu, F.D.; Andraș, A.; Virág, Z.; Brînaș, I.; Draica, M.-I. A Thermo-Mechanical Stress Based Fatigue Life Evaluation of a Mine Hoist Drum Brake System Using COMSOL Multiphysics. *Materials* **2022**, *15*, 6558. https://doi.org/10.3390/ma15196558

[7]. Wolny, S. Loads experienced by load-bearing components of mine hoist installations due to random irregularities and misalignments of the guide string. *J. Mach. Constr. Maint.-Probl. Eksploat.* **2018**, *3*, 79–86.

[8]. Popescu, F.D. *Instalaţii de Transport pe Vertical*; Editura Focus: Petroșani, Romania, 2010.

[9]. Zhang, S.; Han, Z.; Hao, Q.; Liu, Y.; Sha, Z.; Ma, F.; Yang, D. Fatigue Life Calculation of High-Power Disc Brake under Thermal-Mechanical Coupling. *IOP Conf. Ser. Mater. Sci. Eng.* **2019**, *692*, 012022.

[10]. Popescu, F.D., *Aplicaţii industriale ale tehnicii de calcul*, Editura AGIR, Bucureşti, 2009.

[11]. Wang, D.; Zhang, D.; Zhang, Z.; Ge, S. Effect of various kinematic parameters of mine hoist on fretting parameters of hoisting rope and a new fretting fatigue test apparatus of steel wires. *Eng. Fail. Anal.* **2012**, *22*, 92–112.